



Production and Characterization of Activated Carbon from Pomegranate Peel for Pharmaceutical Waste (Paracetamol) Removal: Response Surface Methodology Application

Alper Solmaz[✉] · Zeynel Abidin Sari ·
Mesut Karta · Talip Turna · Ayşegül Yücel ·
Tolga Depci

Received: 9 July 2023 / Accepted: 12 September 2023 / Published online: 5 October 2023
© The Author(s), under exclusive licence to Springer Nature Switzerland AG 2023

Abstract In this study, the goal was to utilize activated carbon (designated as PPAC) derived from pomegranate peel (PP) for the removal of paracetamol (PCM). The distinctive structure of PPAC activated with KOH at 800 C was characterized by X-ray diffraction (XRD), Brunauer–Emmett–Teller (BET), Fourier transform infrared spectroscopy (FTIR), and Scanning Electron Microscope (SEM), revealing a surface area of 692.07 m²/g and a pore diameter of 0.429 cm³/g. Response surface methodology (RSM) was used to determine the relationship between

input parameters such as PCM concentration, PPAC amount, time, pH and temperature parameters and the resulting PCM concentration output. Eight kinetic models and seven isotherm models were examined and compared. As a result, a PCM removal capacity of 214 mg/g was attained, with the most fitting kinetic model being Pseudo Second-Order (R^2 : 0.997) and the most suitable isotherm model being Redlich–Peterson (R^2 : 0.999). According to the Response Surface Methodology (RSM) results, the most effective parameters are time, PPAC amount, initial PCM concentration and pH, respectively. This investigation provides substantial evidence for the viability of utilizing PPAC as an economical and efficient adsorbent in PCM removal processes.

Supplementary Information The online version contains supplementary material available at <https://doi.org/10.1007/s11270-023-06641-w>.

A. Solmaz (✉) · A. Yücel
Department of Environmental Protection
and Control-Iskenderun Vocational School of Higher
Education, Iskenderun Technical University, Hatay, Turkey
e-mail: alper.solmaz@iste.edu.tr

Z. A. Sari · M. Karta
Department of Metallurgy-Iskenderun Vocational School
of Higher Education, Iskenderun Technical University,
Hatay, Turkey

T. Turna
Department of Parks and Garden Plants-Diyarbakır
Vocational School of Higher Education, Dicle University,
Diyarbakır, Turkey

T. Depci
Department of Petroleum and Natural Gas Engineering,
Iskenderun Technical University, Hatay, Turkey

Keywords Pomegranate peel · Activated carbon ·
RSM · Adsorption · Paracetamol removal ·
Pharmaceuticals

1 Introduction

Pharmaceutical drugs encompass bioactive compounds that induce alterations in physiological functions, primarily within human and animal organisms. These are used in disease diagnosis, treatment, and prevention stages (Gómez-Oliván et al., 2014). The wastes generated during the production of drugs are considered industrial waste. After the requisite treatment standards are met within pharmaceutical manufacturing facilities,

it is discharged to the sewage systems in the region where it is located. Furthermore, residual pharmaceutical compounds also enter sewage systems through human use. These drug residues reaching the wastewater treatment plant should not exceed a certain dose (Ahmadfazeli et al., 2021; Li et al., 2021; Phong Vo et al., 2019). Nonetheless, it is well-known since almost all conventional wastewater treatment plants in the world are designed to purify macronutrients, and pharmaceutical wastes can be partially treated in these wastewater treatment plants. Most of them directly reach the receiving environment (lake, pond, river, sea, etc.) from the wastewater treatment plant (Wu et al., 2012). Two of the most significant pharmaceutical compounds encountered in aquatic ecosystems worldwide are PCM (acetaminophen) and acetylsalicylic acid (Lourenção et al., 2009; Phong Vo et al., 2019). The mean concentration of PCM detected at the inlet of a municipal wastewater treatment plant in southeastern Spain has been reported to be 134 µg/L (Gómez et al., 2007; Meinan et al., 2022). Concentrations of up to 65 µg/L were found in another study (Tyne River, UK) (Roberts & Thomas, 2006). Furthermore, PCM's presence has been documented in various water bodies across multiple European countries (Pi et al., 2017; Žur et al., 2018).

Advanced oxidation processes (Dhibi et al., 2023; Nadour et al., 2019), UV degradation (Vaiano et al., 2018), ultrasonic degradation (Soltani et al., 2019), electrochemical degradation (Zhou et al., 2021), reverse osmosis (Lee et al., 2022), and adsorption (Macías-García et al., 2019) are used for treatment of PCM-contaminated water before it reaches sensitive receiving environments. However, in removal studies with oxidation processes, some by-products (low molecular weight compounds) can cause secondary pollutants to be produced (Yun et al., 2019). In addition, some of these treatment methods have disadvantages such as high cost and solid (e.g., sludge) formation (Farooq et al., 2021; Yun et al., 2019). Among them, researchers have shown increasing interest in the adsorption technique as it is a low-cost, flexible, low-energy, and high-efficiency process (Dotto & McKay, 2020; Spessato et al., 2019; Zarroug et al., 2022). Therefore, adsorption can be considered a green and promising approach for the efficient removal of various pollutants present within the aqueous receiving environment.

AC is one of the most widely used adsorbents in the adsorption process. It has a structure with a very large pore size and surface area and high surface reactivity.

AC, which is produced from the end products (wastes) of many industrial and agricultural activities, is widely used to purify various pollutants. Various agricultural by-products such as rice, maize, bananas, flowers, and sugarcane pulp have been used to produce AC. (Ahmed, 2017; Gayathiri et al., 2022). The high-efficiency and low-cost materials that can be used with simple technology are required to remove pollutants from pharmaceutical waste. Recently, researchers have turned their attention to better, readily available, but cheaper materials for generating AC (Danish et al., 2018). On the other hand, as it is known in the treatment studies with AC, many parameters are effective in the treatment efficiency. Some of those include temperature, solution pH, the concentration of the pollutant to be removed at the beginning of the reaction, the amount of adsorbent used, and the contact time between the adsorbent and the pollutant. It is very difficult to express the negative effect of experimental studies, in which many variables are dominant in terms of time and cost and the relationship between the selected parameters. Although there are many mathematical models and software studies to prevent this, the most notable one is RSM (Bashir et al., 2015; Shokoohi et al., 2018). RSM enables the exploration of causal relationships among numerous input variables and output parameters, facilitating the determination of effects and relative weights among these factors. The robustness of this methodology, which has gained considerable traction in water and wastewater treatment applications in recent years, has been substantiated (Garba et al., 2019; Nayeri & Mousavi, 2020).

It is estimated that pomegranate production exceeds four million tons annually (Hernández et al., 2012; Kahramanoglu, 2019). This production is mostly used in the production of fruit juice and jam. Moreover, pomegranate pulp constitutes 30% of the overall fruit weight (Ben-Ali, 2021). Given these figures, if a rough evaluation is made, it means that approximately 1 million 200 thousand tons of pomegranate waste is generated annually. Consequently, these bioresources should be used in their raw form or modified by various processes and reused as much as possible. Thus, if the large amount of organic waste is transformed into valuable products such as AC instead of being waste, various types of contaminants can be adsorbed on this AC with the generation of AC with a large surface area (Karri & Sahu, 2018; Zarroug et al., 2022).

In this study, PPAC derived from pomegranate peel waste was explored as a potential adsorbent for the removal of PCM from aqueous environments. Surface and pore area assessments of the resultant PPAC were carried out via BET analysis under a nitrogen (N_2) gas atmosphere. Furthermore, SEM and FTIR analyses were conducted to elucidate the structural morphological properties, with XRD analysis employed to determine the crystal structure. The outcomes were evaluated utilizing eight kinetic models and seven distinct isotherm models.

2 Material and Method

2.1 Chemicals

All of the chemicals we used during the experiment are of analytical purity. Distilled water was used to prepare the solutions of the chemicals used. In addition, 0.01 M H_2SO_4 and NaOH were used to adjust the pH of the solutions. In the experiment, paracetamol with the formula $C_8H_9NO_2$, which is the active ingredient of more than 600 drugs, CAS number 130–90-2, molecular weight 151.165 g/mol, water solubility at 20 °C 14 g/L, pKa value 9.53 was used. It was obtained from the local pharmacy in liquid form, dissolved in distilled water, and used as a stock solution (Bauer et al., 2021).

2.2 Product of PPAC

During the AC production process, PP was dried at 105 °C for 24 h. Then, the dried biomass was subjected to carbonization for 1 h in a cylindrical furnace (MSE Furnace) at 10 °C/min at 800 °C in the presence of N_2 gas. The carbonized products obtained were activated with 1/4 of the mass of KOH. Then, it was kept at 800 °C for 1 h in the presence of 10 °C/min N_2 gas. The obtained material was treated with 0.5 M HCl to remove inorganic ions. Then, it was washed with distilled water until the pH reached around 7.00, then dried at 100 °C for one night, then left in a desiccator to make it ready for use. Potassium salts such as KOH and K_2CO_3 have been widely used in the manufacture of AC, most commonly using KOH. It has been found that AC prepared by KOH is highly microporous with higher specific surface area (Kim et al., 2021). According to a study conducted by Elmouwahidi et al. (2017), KOH activation produced activated carbon with higher surface area and porosity than phosphoric acid (H_3PO_4) activation (Elmouwahidi

et al., 2017). This was also similar in comparison with sodium hydroxide (NaOH) activation (Saad et al., 2020) on which KOH activation produced incredibly higher BET surface area. It also provides the formation of –OH functional groups. Because K ions (metal) mix into the carbon network and thus carbon loss accelerates, causing the development of pores. For this reason, KOH was used in our study (Solmaz et al., 2023).

2.3 Central Composite Design (CCD) with the Help of RSM

Minitab® 19.2020.1 (64-bit) (Minitab, LLC in the USA) provided by Minitab, LLC in the USA was employed in conjunction with the Central Composite Rotatable Design (CCRD) within the Response Surface Methodology (RSM) framework. This entailed executing a total of 46 experiments, incorporating 5 factors, 1 basic block level, and an iterative approach, with an additional 6 center points. The variables inputted into the program are presented in Table 1. Although there are many models among the RSM methods, the CCD model was used in the removal experiments on PCM. This model requires more experiments than others, depending on the number of factors selected with the whole version step. In addition, it was deemed appropriate to work with this method in terms of allowing experiments to be carried out outside the examined parameter ranges. Within the CCD model, a weighted average value is determined for the investigated parameter, and it is a design method that allows other values to be examined around it.

On the flip side, the results obtained from the study on PCM removal were operated within the RSM, and the results were statistically evaluated. Here, the model fit of the RSM experiments was examined, and the results were presented with three-dimensional-contour graphics. The solutions obtained under the experimental conditions

Table 1 Variables entered in RSM and their values

Variables	Levels				
	$-\alpha$	-1	0	1	$+\alpha$
X1, time (min)	10	0	10	20	30
X2, initial PCM conc. (mg/L)	172.5	10	192.5	375	557.5
X3, AC amount (g)	0.85	0.1	1.05	2.0	2.95
X4, temperature (°C)	15	25	35	45	55
X5, pH	3	2	7	12	17

prescribed by RSM were analyzed, and the amount of PCM removed from the solution was calculated. Subsequently, the PCM percentages removed from the solution were entered as data into the RSM program to model the removal study. In the process of model creation, priority was accorded to experimental conditions yielding maximal PCM removal. Furthermore, through the application of the acquired data within the program, the intricate interplay between each parameter was unearthed and presented via the Analysis of Variance (ANOVA) table, thereby providing insights into their mutual interactions. The statistical significance of the independent variables' influence on the outcomes was determined by assessing the p -values in the generated ANOVA tables. A p -value of ≤ 0.05 denoted a substantial impact of the independent variables on the results.

The statistical validation was reinforced by the utilization of the correlation coefficient (R^2), which is one of the parameters showing second-order model fit according to ANOVA values. The difference between the results obtained according to the specified model and the estimated values generated by the model is called residual, and their results are given collectively in a separate graph. Additionally, the model-provided regression equation was articulated, and the congruence between projected operating points and actual values was ascertained through graphical representation.

2.4 Adsorption Studies

Adsorption investigations were carried out in five stages. In the initial step, PCM solutions with different initial concentrations (93.75, 187.50, 375.00, and 750 mg/L) were prepared from 750 mg/L stock PCM solution in a volume of 100 mL. A contact time of 24 h was provided by adding 100 mg of PPAC obtained from pomegranate peel to these solutions. When the time was completed, UV–Vis measurements were made with the filtrate taken from the 0.45 μm PP membrane filter. Measurements were made at a wavelength of 242 nm. The PCM removal efficiencies obtained using Eq. 1 were calculated as 99.99%, 99.82%, 78.02%, and 37.77%, respectively. According to the results obtained, another study was conducted with PCM solution with a concentration of 281.5 mg/L between 187.50 and 375.00 mg/L with the same conditions. The PCM removal efficiency obtained at this value (Eq. 1) was 59.28%. In the continuation of the study, PCM was continued with 281.5 mg/L as the initial concentration.

Subsequently, within the subsequent step, specific amounts of PPAC (12.5, 25, 50, 100, and 200 mg) were added into the 100 mL solution with an initial concentration of 281.5 mg/L and mixed at 150 rpm for 24 h. Corresponding to the findings obtained under the same filtration conditions, the PCM removal efficiency was calculated as 14.82%, 15.29%, 34.97%, 59.28%, and 97.1%, respectively (Eq. 1). One hundred milligram PPAC was preferred to achieve the highest removal rate with the least amount of PPAC.

The other adsorption parameter is pH. Up to this stage, adsorption studies were carried out at the pH of the solutions (7.05). At this stage, the solution pH was adjusted by using 0.1 M NaOH and 0.1 M HCl. The resultant adsorption efficiencies attained through the experiments performed at pH 3.00 and pH 11.00 were calculated as 30.13% and 27.81%, respectively. For this reason, it was decided to study the solution at its pH in time-dependent adsorption studies. Bernal et al. (2017) reported that they provided the highest removal of paracetamol at pH 7 in their study (Bernal et al., 2017). A time study was performed at the determined optimum conditions (281.5 mg/L, 100 mL, 100 mg PPAC, pH 7.05) (0, 0.5, 1, 3, 5, 10, 15, 30, 45, 60, 90, 120 min). Through this endeavor, it was observed that equilibrium in adsorption was attained at the culmination of 20 min. In order to determine the effect of temperature at optimum conditions, adsorption experiments were carried out at 25, 35, and 45 °C. Upon analysis of the acquired data, it was evident that temperature held negligible impact over the PCM adsorption process.

After the initial PCM concentration (281.5 mg/L) and the amount of pomegranate peel PPAC to be used (1000 mg/L) were determined, the contact time was determined by taking measurements at certain time intervals. According to the results, the adsorption mechanism was tried to be explained with isotherm and kinetic models. The removal efficiency (R) is given in Eq. 1. When the adsorption is in equilibrium, the amount of PCM removed per unit adsorbent (q_e) was calculated with the help of Eq. 2.

$$R(\%) = \frac{C_0 - C_e}{C_0} \times 100 \quad (1)$$

$$q_e = \frac{(C_0 - C_e) \times V}{m} \quad (2)$$

where C_0 and C_e are the initial and equilibrium concentration (mg/L) of PCM, respectively, m adsorbent amount (g), and V is the total volume of solution (L).

2.5 Adsorption Kinetics

To assess the efficacy of the adsorbent, a range of kinetic models were employed. The accurate comprehension of the underlying physical implications and the utilization of standardized solution methodologies for adsorption kinetic models hold paramount significance in ensuring the applicability of these models (Wang and Guo, 2020). The absorption behavior between a solution with an initial concentration and the amount of adsorbent has been tried to be explained by time-dependent kinetic models. The kinetic models used to interpret the experimental studies are presented in Table S1.

2.6 Adsorption Isotherms

The process of adsorption is inherently tied to surface interactions. Trying to explain adsorption data with isotherm models is a widely used method. Adsorption isotherm models can provide information about the maximum adsorption capacity, which is essential in evaluating the performance of adsorbents. The isotherms used to interpret experimental studies are presented in Table S2.

3 Results and Discussion

3.1 Characteristic of PPAC

3.1.1 Textural Characteristics of Adsorbents

The specific surface area of the adsorbent was ascertained using the BET method (TriStar II Plus 3.02). Total surface area, pore volume, and pore size are presented in Table S3. Inherent to any adsorbent particle are pores of diverse dimensions. Subsequently, it was deduced that the structure exhibited mesopores, which fall within the radius range of 1–25 nm. Here, the structures that give the adsorbent adsorbing capacity are micro and mesopores.

On the other hand, gas adsorption has emerged as one of the most used methods to determine the surface area and pore size distributions of powder and porous materials. The nitrogen adsorption/desorption

isotherm of the adsorbent obtained in this direction is presented in Fig. S1. Notably, it was determined that the adsorption/desorption slope increased continuously with the increase of the relative pressure. As defined by the IUPAC (International Union of Pure and Applied Chemistry) classification, distinct adsorption isotherm types are established to align with various pore classifications. The isotherm in Fig. S1 conforms to the type IV adsorption isotherm. In consequence, adsorption at high relative pressures occurs in mesopores, not on open surfaces. Due to the increase in pressure, desorption occurs, and hysteresis formation is observed. The type IV isotherm follows the same path as the type II isotherm for a mesoporous solid in the initial part of the isotherm or with a pore diameter between 2 and 50 nm. It runs parallel to the pressure axis if it is close to the saturation pressure.

3.1.2 Scanning Electron Microscopy (SEM)

SEM images of the activated carbon (PPAC) derived from pomegranate peel are conspicuously illustrated in Fig. 2A, captured using the Thermo Fisher Scientific Apreo S instrument. After PCM removal, and SEM images were retaken (Fig. 2B). The image presented in Fig. 2A is the porous structure of PPAC before adsorption. In Fig. 2A, pores of varying diameters were detected on the surface and internal structure of PPAC. The image shows that the porosity is not macrodimensional; it is developed both on the outer surface and significantly on the inner parts. The resulting structure shows the presence of mezzo and micropores rather than macropores. On the other hand, the SEM image after PCM adsorption is presented in Fig. 2B. The SEM image (Fig. 2B) of the PPAC surface after the PCM adsorption revealed changes in the surface morphology. This transformation is understood to signify the adsorption of PCM within the surface pores.

3.1.3 Surface Functional Groups on the Adsorbents

Pomegranate peel (PP) inherently possesses surface functional groups including lignin, cellulose, and hemicellulose, –OH, –COH, petkin, and amide (Ramutshatsha-Makhwedzha et al., 2022). In addition, fixed carbon ratios are very high, and they have a porous structure (Bhatnagar et al., 2009). FTIR (Jasco-FT/IR-6700) analyses were performed to determine the structural

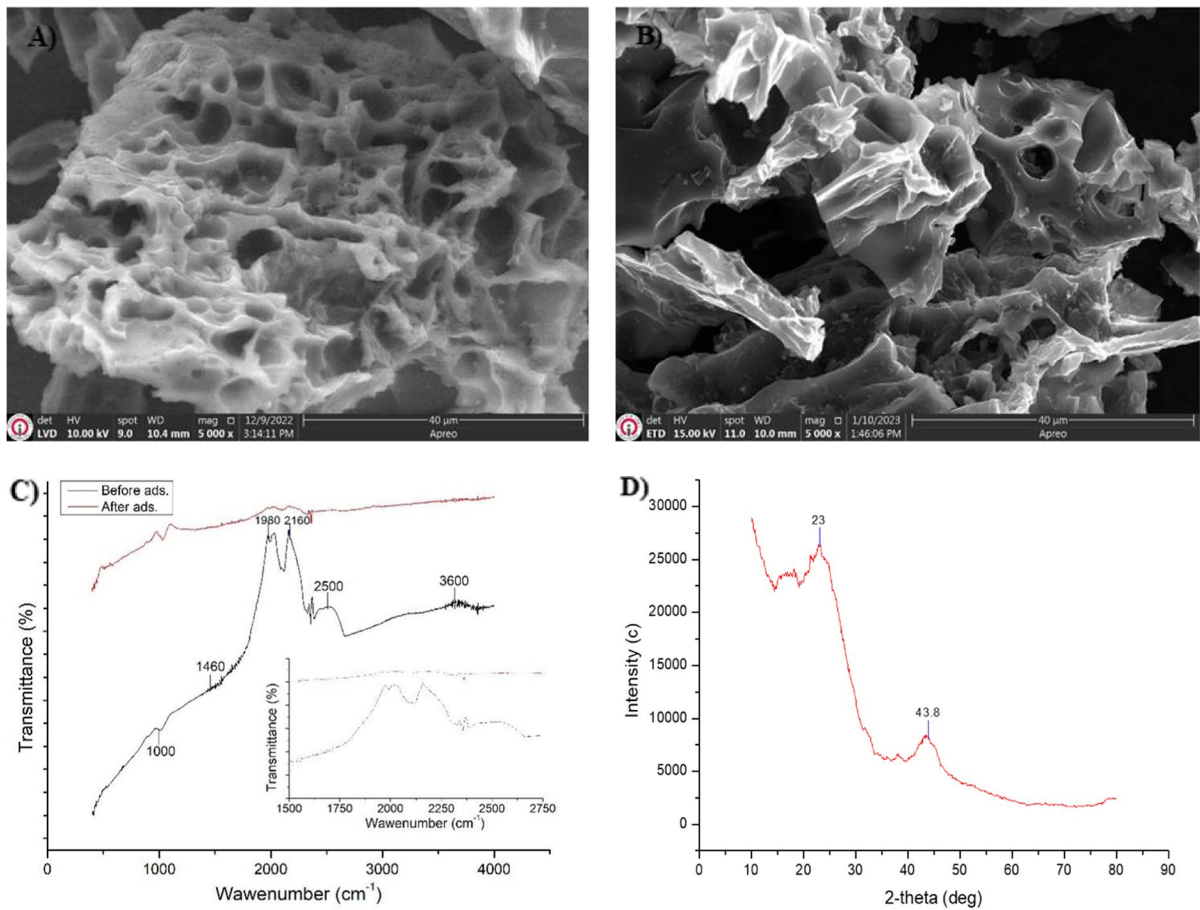


Fig. 1 SEM (5000 \times) images of PPAC before (A) and after adsorption (B), FTIR spectra of the PPAC (C), and the X-ray diffraction pattern of PPAC (D)

changes in PPAC samples produced under the most suitable conditions by chemical activation. The FTIR analyses encompassed both pre- and post-adsorption states, and the comparative results are elucidated in Fig. 1C. With this method, the changes in functional groups were tried to be determined qualitatively. The peaks of PPAC seen at a wavelength of 1000–1300 cm^{-1} , according to Fig. 1C generally indicate that C–O, P=O, P–O–C-, and P=O–OH groups are present. However, it is not clear which group formed. The band observed between 1460 cm^{-1} can be attributed to C–O stretching vibrations (Zhang et al., 2015). The vibration peaks observed in the 1900–2200 cm^{-1} range are in harmony with the methylcellulose peaks. The bands' 2200–2500 cm^{-1} peaks indicate phosphorus (P–H) groups. The peaks observed in the band range of 2840–3000 cm^{-1} indicate the presence of aliphatic structures. It is known that small peaks

observed in the band range of 3200–3600 cm^{-1} express hydroxyl (O–H) groups. Structures containing hydroxyl are phenols, alcohols, and carboxylic structures (Puziy et al., 2005). On the other hand, it was observed that the peak intensities changed between 1500 and 2750 cm^{-1} post absorption. The new peaks formed are predicted to originate from PCM molecules (Chanda et al., 2015; Jyothirmayee et al., 2015).

3.1.4 X-Ray Diffraction (XRD) Analysis

The process of chemical activation and carbonization employed in the production of PPAC induces significant alterations in the substance's molecular, crystalline, and biomass. For this reason, XRD is one of the commonly used methods to determine the characterization features of this changing structure. Accordingly,

the crystal structure of PPAC was analyzed by XRD (Rigaku, Miniflex 600). The XRD chart is presented in Fig. 1D. As can be seen from the figure, amorphous structures were obtained for the synthesized materials. In particular, the various small-sized peaks seen in the figure are due to the mineral remaining due to the activation process with KOH used in AC production (Al-Qodah & Shawabkah, 2009). Also, the peaks at about $2\theta=23^\circ$ and 43.8° can be attributed to the planes of hexagonal graphite (002 and 101). Furthermore, the increase in the density of low-angle scattering peaks confirms the high micropore density in the material (Qian et al., 2013). This increases the adsorption capacity of PPAC. On the other hand, the peaks seen at $2\theta=25^\circ$ and 43° are considered crystal structures in PPAC (Omri et al., 2013).

3.2 Central Composite Design (CCD)

3.2.1 Model Fitting and Statistical Evaluation

The experimental design created with the help of the model and the results of the experiments performed according to this design are presented in Table S4. Concomitantly, the ANOVA analyses of the experiments performed as a result of the RSM design are exhaustively detailed in Table 2, and the model summary is presented in Table 3. Furthermore, the graph obtained from the values estimated in the regression model against the results obtained in the experimental studies is presented in Fig. S2.

As it is known, the regression equation (R^2) shows the agreement between the data obtained from the

Table 2 ANOVA (Analysis of Variance) models for PPAC of PCM

Source	DF	Adj SS	Adj MS	F-value	P-value
Model	20	51518.9	2575.9	9.86	0.000
Linear	5	32563.9	6512.8	24.93	0.000
Time (min)	1	17033.5	17033.5	65.19	0.000
Initial PCM conc. (mg/L)	1	1551.2	1551.2	5.94	0.022
AC amount (g)	1	12571.1	12571.1	48.11	0.000
Temperature ($^\circ\text{C}$)	1	25.8	25.8	0.10	0.756
pH	1	1382.3	1382.3	5.29	0.030
Square	5	14875.5	2975.1	11.39	0.000
Time (min)*Time (min)	1	12971.1	12971.1	49.65	0.000
Initial PCM cont. (mg/L)*Initial PCM cont. (mg/L)	1	93.9	93.9	0.36	0.554
AC amount (g)*AC amount (g)	1	3239.5	3239.5	12.40	0.002
Temperature ($^\circ\text{C}$)*Temperature ($^\circ\text{C}$)	1	234.3	234.3	0.90	0.353
pH*pH	1	1247.0	1247.0	4.77	0.039
2-Way Interaction	10	4079.5	407.9	1.56	0.176
Time (min)*Initial PCM cont. (mg/L)	1	1.4	1.4	0.01	0.942
Time (min)*AC amount (g)	1	1093.9	1093.9	4.19	0.051
Time (min)*Temperature ($^\circ\text{C}$)	1	7.6	7.6	0.03	0.866
Time (min)*pH	1	1408.2	1408.2	5.39	0.029
Initial PCM cont. (mg/L)*AC amount (g)	1	13.2	13.2	0.05	0.824
Initial PCM cont. (mg/L)*Temperature ($^\circ\text{C}$)	1	152.6	152.6	0.58	0.452
Initial PCM cont. (mg/L)*pH	1	47.5	47.5	0.18	0.674
AC amount (g)*Temperature ($^\circ\text{C}$)	1	810.3	810.3	3.10	0.090
AC amount (g)*pH	1	10.5	10.5	0.04	0.843
Temperature ($^\circ\text{C}$)*pH	1	534.3	534.3	2.05	0.165
Error	25	6531.9	261.3		
Lack-of-Fit	20	6478.3	323.9	30.23	0.001
Pure Error	5	53.6	10.7		
Total	45	58050.8			

Table 3 Model summary for PCM removal

S	R-sq	R-sq(adj)
16.16	88.75%	79.75%

experimental results. Moreover, the compatibility of the estimated values with the experimental studies is also essential in terms of the suitability of the study. Accordingly, the R^2 value of our study was found to be 88.75%, while the consistency of the values obtained from the experimental studies was 92.5%. In parallel, the model's F -value was determined as 9.86. In the literature, chromium (VI) removal with AC was found to be 96.59%, while the F -value was calculated as 31.52 (Anupam et al., 2011). In another study, in which AC and COD and color removal from bananas were made, R^2 values were found to be 83.94–93.23%, while F -values were reported as 6.67–22.74%. When the R^2 value and F -values, in which the model fit is proven, are examined, the results obtained in our study are pretty reasonable compared to the model estimation results.

In adsorption studies, T - and P -values, one of the most basic indicators, should be examined to determine the net relationship between the input parameters and the response parameter. The + or – sign in the parameters' reputation indicates a positive (synergistic) or negative (antagonistic) effect. Here, especially if the P -value is less than 0.005, the relationship between the response parameter and the input parameter is considered high (Dolatabadi & Ahmadzadeh, 2019). In our study, the most critical parameters affecting the PCM removal efficiency were “time” and “AC amount.” At the same time, the “initial PCM concentration” and “pH” parameters also affected significantly, but it was seen that the effect of temperature was lower than the other parameters.

It is seen that the Adj- R^2 value (88.75%) is lower than the actual R^2 value (79.75%) throughout the study. Considering the number of terms in the sample and the model size, this situation can be considered normal (Box & Behnken, 1960). Also, the values showing the differences between the observed values and the predicted values in our study, namely

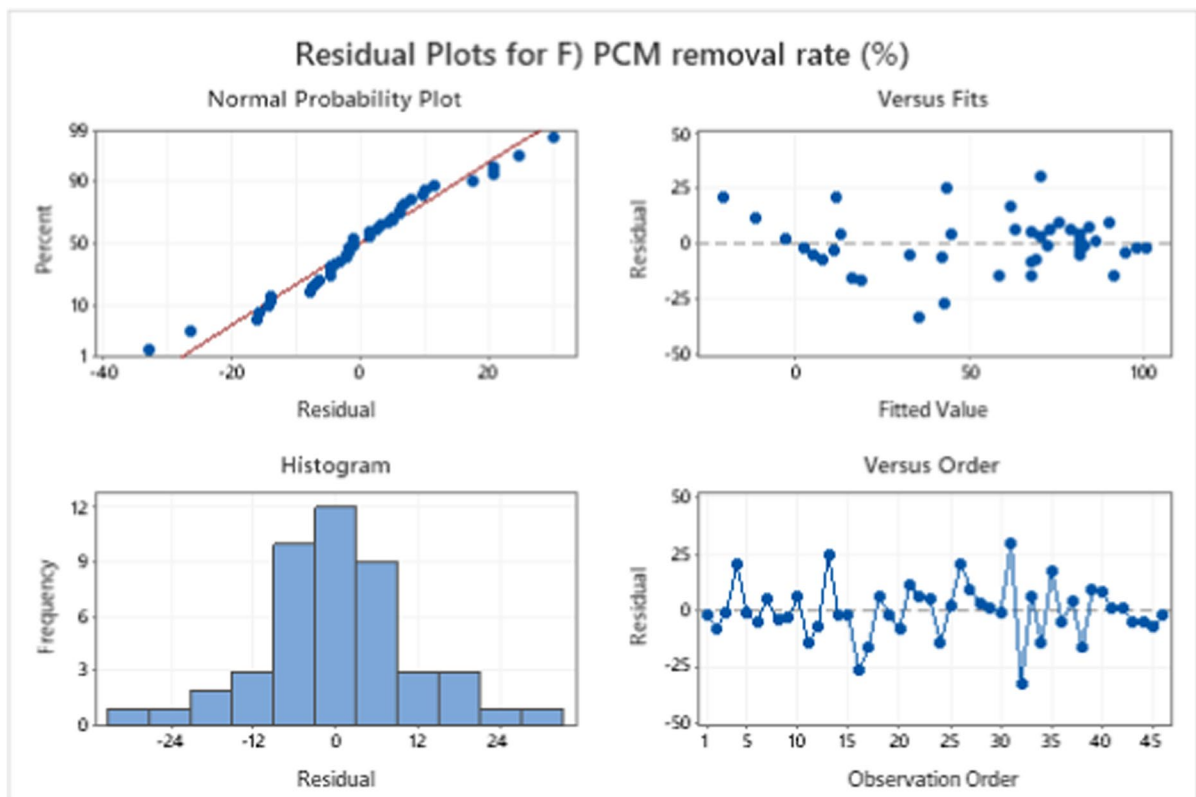


Fig. 2 Residue values plots for PPAC, **a** normalized percentage vs. residual values, **b** fixed percentage vs. residual value, **c** residual vs. frequency, **d** residual vs. observation pattern

“residual values,” are calculated and presented in Fig. 2.

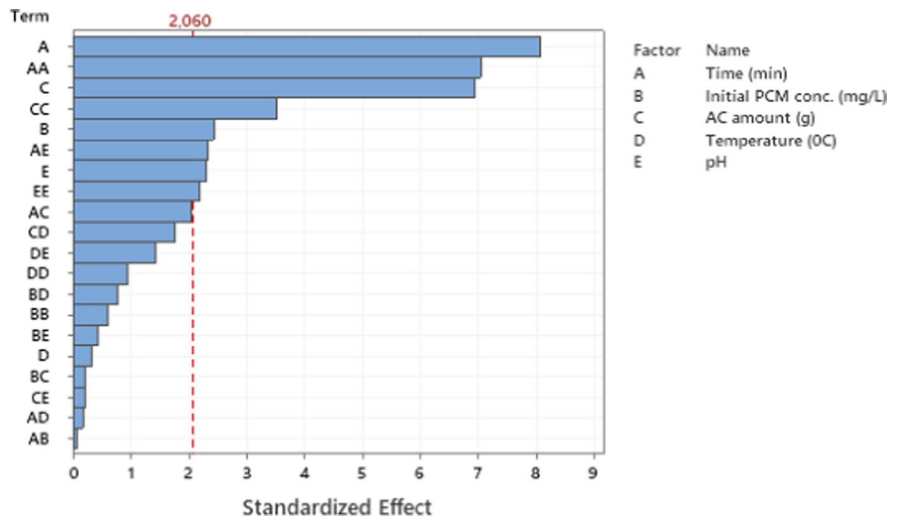
Residue/residual values can be defined as numbers that cannot be expressed in the model. Even the distribution of these values is expected to be within normal limits. That is, the points in the normal probability graph are expected to be as close to a straight line as possible. Some deviations together may not cause significant variability in results. Again, when the histogram graph is viewed as left and right according to the average value, there are expected to be no contradictions and most of it will be close to zero (Danmaliki et al., 2017). Therefore, no discrepancy is observed in our study’s residual data distribution.

3.2.2 Modeling of the Adsorption Process

The empirical model equation used to reach the estimated values is as follows:

$$\begin{aligned}
 \text{PCM\%} = & -100 + 16.42A - 0.116B + 0.1C \\
 & + 3.03D + 17.05E - 0.6854A * A \\
 & - 0.000098B * B - 21.35C * C \\
 & - 0.0518D * D - 0.478E * E - 0.00044A \\
 & * B + 2.32A \& C - 0.018A * D \\
 & - 0.500A * E + 0.0105B * C \\
 & + 0.00338B \& D - 0.00378B * E \\
 & + 1.498C * D + 0.34C * E - 0.231D \\
 & * E
 \end{aligned}$$

Fig. 3 Pareto charts for PCM removal by PPAC



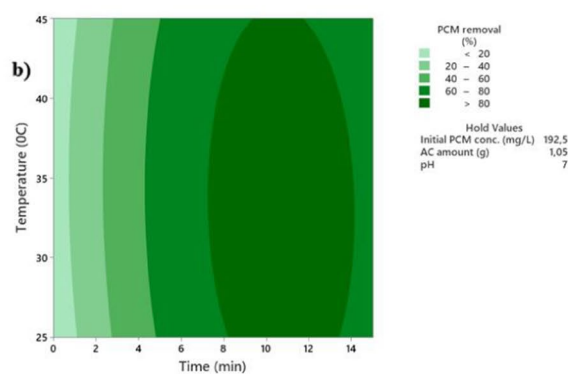
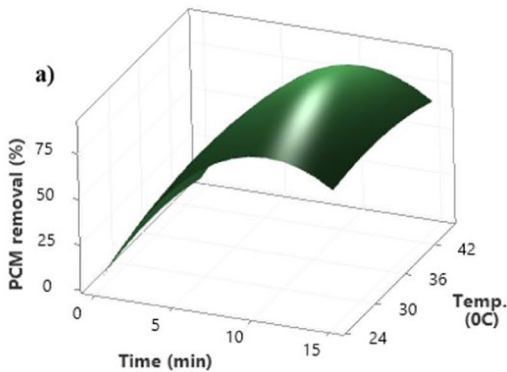
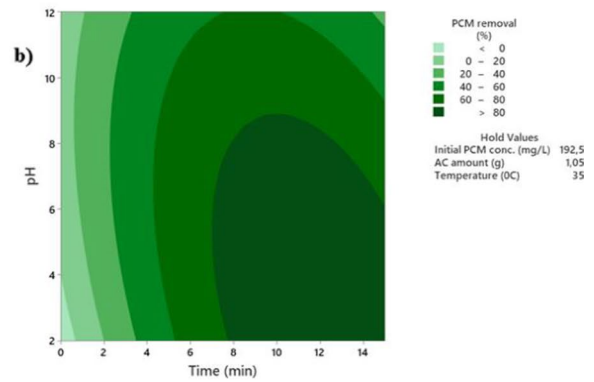
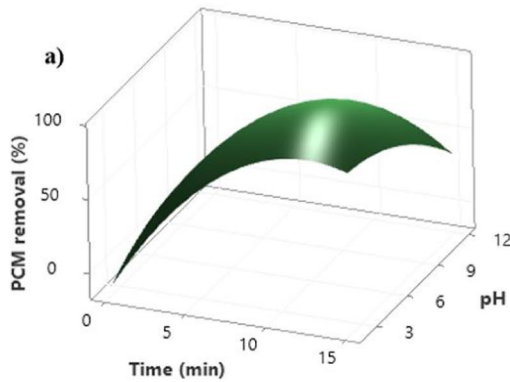
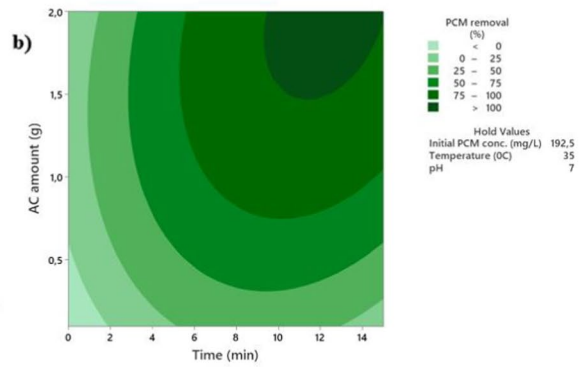
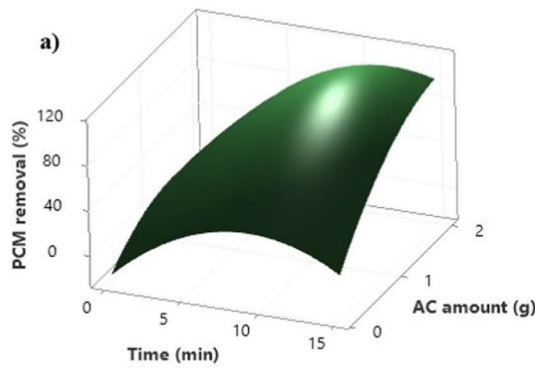
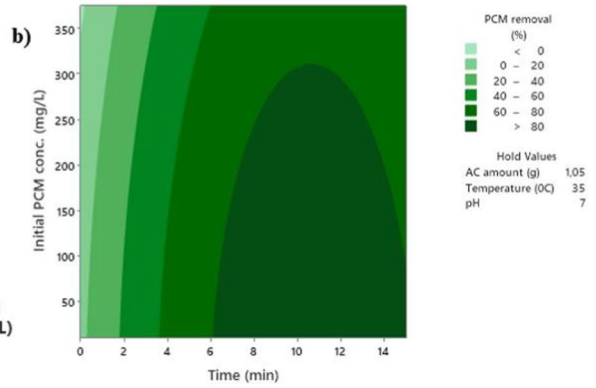
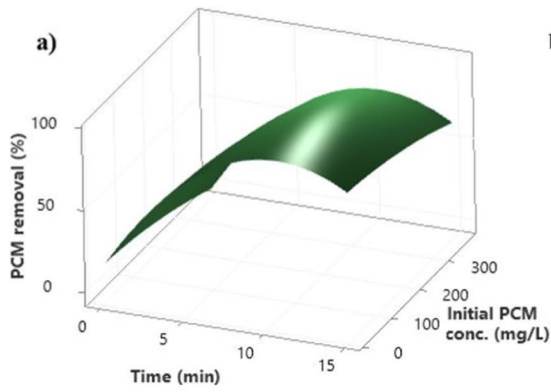
Here, *A* is time (min), *B* is Initial PCM concentration (mg/L), *C* is amount of AC (g), *D* is temperature (°C), and *E* is pH. The relationship table between the mentioned inputs and the response variable is shown in Table S5.

The Pareto chart showing the standardized effects of the inputs and the response variable is presented in Fig. 3.

Again, similar to the ANOVA analysis, as seen from the Pareto charts, the most critical parameter effective on PCM removal is “time.” This is followed by “PPAC amount,” “initial PCM concentration,” and “pH.” On the other hand, the effect of the “temperature” parameter is lower than the others. Considering these parameters’ quadratic and cross effects, the time parameter stands out, but the amount of PPAC seems to be quite effective on the PCM removal efficiency.

3.2.3 Effect of Key Factors as Surface Plots and Counterplot

Figure 4 shows response surface plots and contour plots of PCM removal efficiencies versus time-dependent variability of initial PCM concentration, AC amount, pH, and temperature. In particular Fig. 4a, it can be observed that the PCM removal efficiency increases with increasing reaction time when pH 7 values are kept constant at 35 °C in the presence of 1.05 g AC. Again, when the contour graph in Fig. 4b part of this graph is examined, the increase in the initial PCM concentration with the reaction time shows that the efficiency increases again.



◀**Fig. 4** The response surface plots (a) and contour plots (b) of the PCM removal efficiency (%) as the function of time (min) vs. initial PCM conc. (mg/L), AC amount (g), pH, and temperature (°C)

3.3 Adsorptive Removal of PCM

3.3.1 Adsorption Kinetics

The phenomenon of adsorption is intrinsically intertwined with the process of adsorbate molecules within a solution binding onto the surface of the adsorbent. While this event occurs on the surface of the adsorbent, it will begin to occur in the meso and micropores later. The kinetic models evaluated within the scope of the study are presented in Fig. 5, and the summary of the numerical values obtained from these models is presented in Table 4. In addition, the graph created for each isotherm is Fig. 5 presented in S3. When Fig. 5 and Table 4 were examined together, it was seen that the adsorption reached equilibrium within 20 min. It was observed that the kinetic models given in Fig. 5 gave similar results. In such cases, a specific adsorption behavior cannot be explained.

The graphical representation of “liquid film diffusion” implies a shift in the adsorption process towards the solid surface. The rate of an adsorption event can be controlled by external, internal, and both types of diffusion (Karthikeyan et al., 2010). Three-step adsorption between PCM ions and the surface of PPAC (Gupta et al., 2003; Park, 1975; Weber and Morris, 1963) may have

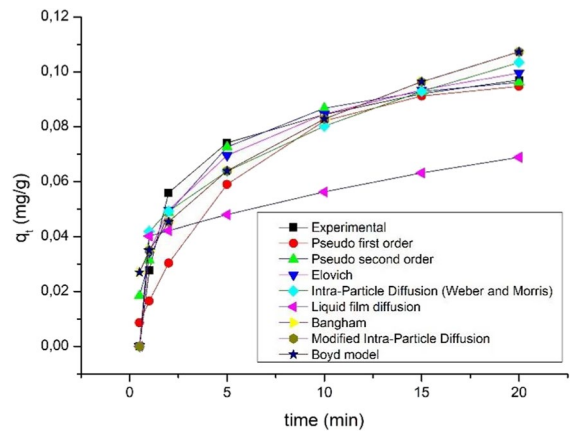


Fig. 5 Comparison of evaluated kinetic models

occurred. The first is that the PCM ions form a film on the surface of the PPAC. In the progressive stage, it is the movement of PPAC towards its pores. Moreover, finally, it is the adsorption action that PCM ions form on the inner surface of PPAC. A discerning examination of the R^2 values identifies the “Pseudo second-order” kinetic model as the frontrunner. When the literature is examined, it has been stated that the adsorption kinetics are suitable for the “Pseudo second-order” model, as in many adsorbent materials, in case the adsorption is in equilibrium and the active site of the adsorbent material is high (Guo & Wang, 2019; Wang and Guo, 2020). This kinetic model is used to predict the behavior of the entire adsorption

Table 4 Summary of data from the kinetic models evaluated

Kinetic models	Pseudo first-order	Pseudo second-order	Battacharya and Venchobacher	Elovich	Intra-particle diffusion	Liquid film diffusion	Bangham	Modified intra-particle diffusion
Parameters	$k_1=0.052$	$k_2=3.826$ $q_e=0.108$	$k_b=-0.046$	$\beta=46.103$ $\alpha=0.107$	$k_i=0.018$ $a=0.024$	$k_{id}=0.037$	$m=2.673$ $k_f=0.035$	$a=0.374$ $k_{id}=0.223$
R^2	0.957	0.997	0.957	0.966	0.879	0.974	0.881	0.881
SSE	0.001	0.000	0.012	0.000	0.000	0.003	0.001	0.000
SAE	0.066	0.035	0.258	0.022	0.043	0.137	0.071	0.044
ARE	16.09	4.67	55.31	6.61	12.72	28.28	10.84	10.84
HYBRID	22.519	0.147	77.432	2.268	5.413	21.814	1.325	1.325
MPSD	0.985	0.937	0.997	0.963	0.971	0.985	0.958	0.958
χ^2	0.019	0.002	0.164	0.003	0.010	0.045	0.007	0.007

R^2 coefficient of determination, *SSE* sum of squares errors, *SAE* sum of absolute errors, *ARE* average relative errors; *HYBRID* hybrid fractional error function, *MPSD* Marquardt’s percent standard deviation, χ^2 non-linear chi-square test.

event. This means that the adsorption rate depends on the adsorbent’s adsorption capacity (Sahoo & Prelot, 2020). This means that the adsorption rate is dependent on the PPAC adsorption capacity, not the PCM concentration.

3.3.2 Adsorption Isotherms

Graphical representations of adsorption isotherm models are often used to elucidate the relationship between the adsorbate and adsorbent in linear fashion, aiding in the distinction between homogeneous and heterogeneous coating-type adsorption (Foo & Hameed, 2010). The Langmuir Isotherm is the situation where maximum adsorption is in a single layer saturated on the adsorbent surface (Agyei et al., 2000). Essentially, it is based on the assumption that there is no chemical interaction between the PCM molecules and the PPAC surface and that the PCM molecules adhere as a single layer on the PPAC surface. The Freundlich isotherm, on the other hand, offers an approach that tries to explain a multilayer heterogeneous adsorption (Baup et al., 2000). With this model, PCM molecules are envisioned as attaching in more than one layer to certain regions of the PPAC surface, accounting for its heterogeneous nature. The Redlich–Peterson (R–P) isotherm has been developed to explain homogeneous and heterogeneous systems. This isotherm is a method that includes the Langmuir and Freundlich isotherms (Foo & Hameed, 2010). Among the investigated isotherm models, the Redlich–Peterson (R–P) isotherm was

Fig. 6 Adsorption isotherms for the removal of PCM, black line **A** Freundlich, **B** Langmuir, **C** Temkin, **D** Halsey, **E** Dubinin–Radushkevich, **F** Harkin–Jura, **G** Redlich–Peterson. The black dots represent the experimental run results, and the red line represents the linearized isotherms

the most suitable model for PCM removal with the help of PPAC. The summary of the calculations for the isotherm models calculated in the study is presented in Table 5, and the graph created for each isotherm is presented in Fig. 6.

3.4 The General Assessment of Removal Efficiencies

Since PCM removal is not performed with AC obtained from PP in the literature, different types of pollutants removed with this AC and studies that are not produced from PP but have PCM removal are compiled and presented in Table 6. In previous studies, it was reported that chemical adsorption occurred in carboxylic groups in which AC and PCM removal were performed, obtained from Jatoba fruits and produced at 500 °C and activated with KOH. The removal efficiency was reached between 113.69 and 356.22 mg/g (Spesato et al., 2019). Similarly, in an investigation involving wastewater treatment plant sludge and commercial ACs, efficient removal of paracetamol was observed through adsorption, with a removal efficiency of 212.26 mg/g. The adsorption process was linked to hydrogen bond interactions (Lladó et al., 2015). Furthermore, it has been reported that AC produced from PP at 500 °C has a surface

Table 5 Summary of data from the evaluated isotherm models

Isotherms	Freundlich	Langmuir	Temkin	Halsey	Dubinin–Radushkevich	Harkins–Jura	Redlich–Peterson
Parameters	$k_F=0.119$ $1/n=0.096$	$k_L=0.089$ $RL=0.981$ $q_{max}=0.214$	$BT=149.71$ $k_T=1023.08$	$n_H=-10.41$ $k_H=0$	$k_D=1.22$ $q_s=0.197$ $E=0.641$	$A_{HJ}=0.062$ $B_{HJ}=3.892$	$\alpha=0.914$ $a_R=6.974$ $k_R=0.878$
R ²	0.965	0.996	0.950	0.965	0.901	0.986	0.999
SSE	0.000	0.001	0.000	0.156	0.000	0.107	0.000
SAE	0.027	0.031	0.028	0.788	0.029	0.643	0.029
ARE	9.8	12.9	10.50	297.40	10.40	296.60	10.4
HYBRID	10.90	25.80	13.39	594.87	11.62	889.73	23.24
MPSD	0.978	0.987	0.980	1.018	0.979	1.022	0.986
X ²	0.004	0.009	0.006	2.289	0.005	1.282	0.005

The explanations of the abbreviations are as in Table 6.

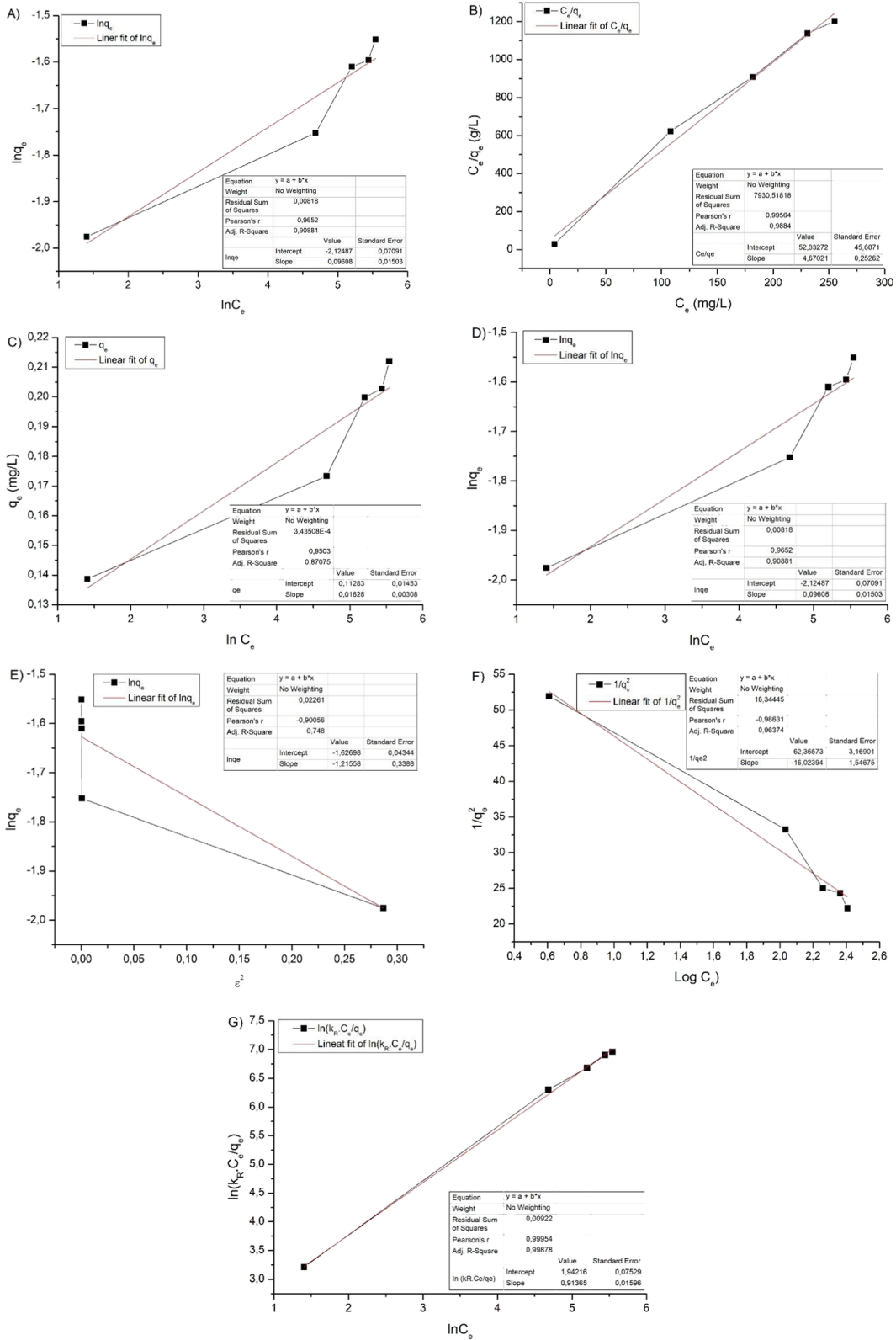


Table 6 Comparison of the obtained values with the literature

	This study	(Saadi et al. 2022)	(Turkmen Koc et al. 2021)	(Senthilkumar et al. 2016)	(Mahdieh Namvar-Mahboub et al. 2020)	(Zarroug et al. 2022)	(Lladó et al. 2015)	(Spessato et al. 2019)	(Tran et al. 2020)	(Sara Tunç et al. 2021)
AC origin	Pomegranate peels	Pomegranate peels	Pomegranate peels	Pomegranate peel	Pomegranate peel	Pomegranate peels	1-Commercial 2-WWTP sludge	Jatoba fruits	Pomelo peel wastes	Wood sawdust
AC preparation chemical	KOH	K ₂ CO ₃	ZnCl ₂ , H ₂ SO ₄	H ₃ PO ₄	H ₂ SO ₄	-	-	KOH	-	H ₃ PO ₄
AC preparation temperature (°C)	800	850, 900, 950	800W microwave	400–600	500	450 °C @ 10 min	-	500	600–900	650 °C @ 60 min
BET-surface area (S _{BET} , m ² /g)	692.07	1.860	-	686	235	1.657	1.234	2794 and 889	1292	96.33
BET-pore volume (cm ³ /g)	0.429	0.879	-	0.505	-	0.91	0.615	-	0.704	0.051
Experiment volume (mL)	10	-	50	-	50	-	250	25	25	100
Mixing speed (rpm)	60–240	-	500	-	180	-	-	-	-	160
Experiment time	20 min	-	2–4 h	73 min	48 h	-	1–48 h	240 min	48 h	-
pH's studied	2.00–11.00	-	-	-	2–12	-	-	3–10	2–11	6.70
Experiment temperature (°C)	25, 35, 45	-	-	-	-	-	25	30–50	10, 25, 50	30
Pollutant removed	PCM	CO ₂ , H ₂ , CH ₄	-	Methylene blue	Pyridine	PCM	PCM	PCM	PCM	PCM
Initial concentrations (mg/L)	281.5	-	40	-	25–200	-	1–150	25–250	517 and 884	5–30
The adsorption capacity of AC (mg/g)	214	717	37.17	169	100	238	212.26	356.22–113.69	286	15.90

Table 6 (continued)

This study	(Saadi et al. 2022)	(Turkmen Koc et al. 2021)	(Senthilkumar et al. 2016)	(Mahdieh Namvar-Mahboub et al. 2020)	(Zarroug et al. 2022)	(Lladó et al. 2015)	(Spessato et al. 2019)	(Tran et al. 2020)	(Sara Tunç et al. 2021)
Adsorbent amount (g)	1	0.25	-	0.1	-	0.05	-	0.05	0.02–0.2

area of 235 m²/g, and it has been reported that 100 mg of Pyridine removal per gram adsorbent is achieved with this AC (Mahdieh Namvar-Mahboub et al., 2020). In a separate study, it was reported that the product produced at 400–600 °C was activated with H₃PO₄ to reach a surface area of 686 m²/g, and the maximum Methylene blue removal efficiency of this AC was 169 mg/g (Senthilkumar et al., 2016). Moreover, Zarroug et al. produced AC with a large surface area from pomegranate peels by microwave method and removed paracetamol from pharmaceutical wastes (Zarroug et al., 2022). In our study, AC was produced at 800 °C and activated with KOH, yielding a surface area of 692.07 m²/g. PCM removal was performed with this AC, resulting in 214 mg PCM removal per gram adsorbent.

3.5 Scale-up Potential and Future Perspectives of PPAC

The innovative approaches have become very popular today, both to eliminate the environmental risks of biodegradable products and to transform these products from waste into a product that will contribute to the economy. Among these, AC production has become quite widespread both scientifically and technologically in terms of ease of use and low operating cost. Many bioproducts such as corn, wheat, grass, coconut, apricot, olive seed, palm, banana rice, and wood have been used in AC production (Yahya et al., 2015). Laboratory-scale AC production involves the use of different chemicals (ZnCl₂, KOH, H₃PO₄, and K₂CO₃) and a variety of high-temperature furnaces or reactors such as microwave ovens or hydrothermal reactors (Ioannidou & Zabaniotou, 2007). By utilizing waste plant products like pomegranate peel, which are abundant in regions like the Mediterranean, not only are waste materials reduced, but they are also transformed into economically viable products. In the removal studies with the obtained AC, many organic and inorganic pollutants are removed from domestic and complex industrial wastes as well as micro and macro pollutants in drinking and utility water (De Gisi et al., 2016; Fu & Wang, 2011). There are various studies available to scale-up laboratory-scale studies and adapt them to real scale. It varies according to the nature of the chemical

used in these processes and the specification of the applied process, and the surface areas of the ACs produced accordingly vary accordingly. In this context, the price of ACs obtained from waste plant products varies in the range of about 0.15–41.92 USD/kg, but it can be stated that it varies between 1 and 2 USD/kg on average (Dadebo et al., 2023a, 2023b; Dadebo et al., 2023a, 2023b; Jaria et al., 2022). Considering the specific pollutants and their concentrations, the cost of pollutant removal per unit of wastewater can vary widely. When the Global AC Market in the world is estimated to be 14.07 billion US in 2027, AC production from waste will increase its popularity in the coming years (Zein & Antony, 2022).

4 Conclusions

In this study, the PCM removal efficiency of AC produced from waste PP was investigated. The results are summarized below:

- In the structural and other characterization analyses of PPAC, it was determined that it has an amorphous structure and a surface area of 692.07 m²/g.
- When the post-adsorption SEM images are examined, there are residues of PCM molecules in some places. In addition, the appearance of different peak intensities in the FTIR analysis post-adsorption analysis proves there will be PCM molecules on the PPAC surface.
- It was measured that the adsorption process reached equilibrium in 20 min, and the amount of pollutant removed per unit adsorbent was 214 mg/g.
- Pseudo Second-Order (R^2 :0.997) and Redlich–Peterson (R^2 :0.999) were found to be the most suitable models, respectively, according to kinetic and isotherm determinations. Thus, it can be assumed that heterogeneous and physical adsorption of PCM molecules on PPAC in the form of diffusion takes place.
- In the Pareto Chart prepared with the data obtained from the experiments performed as a result of the RSM design, it was seen that the three most important factors were time, initial PCM concentration, and amount of activated carbon.

- Considering the relationship between these three parameters, it was observed that the highest removal efficiency was reached between 10 and 14 min when the initial PCM concentration was 250–300 mg/L, and the PPAC amount was between 1.5 and 2 g. When the results of RSM modeling and experimental studies are compared, it is seen that the results overlap with each other.

According to these results, it was observed that PPAC obtained from waste PP is a potential adsorbent material in the removal of high-concentration pharmaceutical wastes (PCM).

5 Data Availability

The datasets generated during and/or analyzed during the current study are available from the corresponding author on reasonable request.

Acknowledgements The authors would like to thank to Iskenderun Technical University for their financial support.

Author Contribution Alper Solmaz and Ayşegül Yücel: they contributed equally to this work. Conceptualization, formal analysis, investigation, data curation, writing—original draft. Zeynel Abidin Sarı: data curation, result interpretation, writing—review and editing. Mesut Karta: original draft, formal analysis, data curation, writing—review and editing. Talip Turna: investigation, writing—review and editing. Tolga Depci: supervision, investigation, writing—review and editing.

Funding This research is partially funded by Iskenderun Technical University (Project Number: 2021LBTP10).

Declarations All authors have read, understood, and have complied as applicable with the statement on “Ethical responsibilities of Authors” as found in the Instructions for Authors and are aware that with minor exceptions, no changes can be made to authorship once the paper is submitted.

Ethical Approval

Not applicable.

Consent to Participate All authors have given consent to their contribution.

Consent for Publication All authors have agreed with the content and given explicit consent to publish.

Competing Interests The authors declare no competing interests.

References

- Agyei, N. M., Strydom, C. A., & Potgieter, J. H. (2000). An investigation of phosphate ion adsorption from aqueous solution by fly ash and slag. *Cement and Concrete Research*, 30(5), 823–826. [https://doi.org/10.1016/S0008-8846\(00\)00225-8](https://doi.org/10.1016/S0008-8846(00)00225-8)
- Ahmadfazel, A., Poureshgh, Y., Rashtbari, Y., Akbari, H., Pournali, P., & Adibzadeh, A. (2021). Removal of metronidazole antibiotic from aqueous solution by ammonia-modified activated carbon: Adsorption isotherm and kinetic study. *Journal of Water, Sanitation and Hygiene for Development*, 11(6), 1083–1096. <https://doi.org/10.2166/WASHDEV.2021.117>
- Ahmed, M. J. (2017). Adsorption of non-steroidal anti-inflammatory drugs from aqueous solution using activated carbons: Review. *Journal of Environmental Management*, 190, 274–282. <https://doi.org/10.1016/J.JENVMAN.2016.12.073>
- Al-Qodah, Z., & Shawabkha, R. (2009). Production and characterization of granular activated carbon from activated sludge. *Brazilian Journal of Chemical Engineering*, 26(1), 127–136. <https://doi.org/10.1590/S0104-66322009000100012>
- Anupam, K., Dutta, S., Bhattacharjee, C., & Datta, S. (2011). Adsorptive removal of chromium (VI) from aqueous solution over powdered activated carbon: Optimisation through response surface methodology. *Chemical Engineering Journal*, 173(1), 135–143. <https://doi.org/10.1016/J.CEJ.2011.07.049>
- Bashir, M. J. K., Tunku, U., Rahman, A., Amr, S. A., & Aziz, S. Q. (2015). Wastewater treatment processes optimization using response surface methodology (RSM) compared with conventional methods: Review and comparative study. *Middle East Journal of Scientific Research*, 23(2), 244–252. <https://doi.org/10.5829/idosi.mejsr.2015.23.02.52>
- Bauer, A. Z., Swan, S. H., Kriebel, D., Liew, Z., Taylor, H. S., Bornehag, C.-G., et al. (2021). Paracetamol use during pregnancy — A call for precautionary action. *Nature Reviews Endocrinology*, 17(12), 757–766. <https://doi.org/10.1038/s41574-021-00553-7>
- Baup, S., Jaffre, C., Wolbert, D., & Laplanche, A. (2000). Adsorption of pesticides onto granular activated carbon: Determination of surface diffusivities using simple batch experiments. *Adsorption*, 6(3), 219–228. <https://doi.org/10.1023/A:1008937210953/METRICS>
- Ben-Ali, S. (2021). Application of raw and modified pomegranate peel for wastewater treatment: A literature overview and analysis <https://doi.org/10.1155/2021/8840907>
- Bernal, V., Erto, A., Giraldo, L., & Moreno-Piraján, J. C. (2017). Effect of solution pH on the adsorption of paracetamol on chemically modified activated carbons. *Molecules*, 22(7), 1032. <https://doi.org/10.3390/MOLECULES22071032>
- Bhatnagar, A., Kumar, E., Minocha, A. K., Jeon, B. H., Song, H., & Seo, Y. C. (2009). Removal of anionic dyes from water using Citrus limonum (Lemon) peel. *Equilibrium Studies and Kinetic Modeling*, 44(2), 316–334. <https://doi.org/10.1080/01496390802437461>
- Box, G. E. P., & Behnken, D. W. (1960). Some new three level designs for the study of quantitative variables. *Technometrics*, 2(4), 455–475. <https://doi.org/10.1080/00401706.1960.10489912>
- Chanda, A., Vikash, B., Dey, A., Gupta, P., Yuvraj, P. K., & Rathnam, G. (2015). Evaluation and isolation of novel binding agent *Alstonia scholaris* in the formulation of tablet. *World Journal of Pharmacy and Pharmaceutical Sciences*, 4, 1247–1258.
- Dadebo, D., Atukunda, A., Ibrahim, M. G., & Nasr, M. (2023a). Integrating chemical coagulation with fixed-bed column adsorption using rice husk-derived biochar for shipboard bilgewater treatment: Scale-up design and cost estimation. *Chemical Engineering Journal Advances*, 16, 100520. <https://doi.org/10.1016/j.cej.2023.100520>
- Dadebo, D., Ibrahim, M. G., Fujii, M., & Nasr, M. (2023b). Sequential treatment of surfactant-laden wastewater using low-cost rice husk ash coagulant and activated carbon: Modeling, optimization, characterization, and techno-economic analysis. *Bioresource Technology Reports*, 22, 101464. <https://doi.org/10.1016/j.biteb.2023.101464>
- Danish, M., Ahmad, T., Majeed, S., Ahmad, M., Ziyang, L., Pin, Z., & Shakeelqubal, S. M. (2018). Use of banana trunk waste as activated carbon in scavenging methylene blue dye: Kinetic, thermodynamic, and isotherm studies. *Bioresource Technology Reports*, 3, 127–137. <https://doi.org/10.1016/J.BITEB.2018.07.007>
- Danmaliki, G. I., Saleh, T. A., & Shamsuddeen, A. A. (2017). Response surface methodology optimization of adsorptive desulfurization on nickel/activated carbon. *Chemical Engineering Journal*, 313, 993–1003. <https://doi.org/10.1016/J.CEJ.2016.10.141>
- De Gisi, S., Lofrano, G., Grassi, M., & Notarnicola, M. (2016). Characteristics and adsorption capacities of low-cost sorbents for wastewater treatment: A review. *Sustainable Materials and Technologies*, 9, 10–40. <https://doi.org/10.1016/J.SUSMAT.2016.06.002>
- Dhibi, H., Guiza, M., Bouzaza, A., Ouederni, A., Lamaa, L., Péruchon, L., et al. (2023). Photocatalytic degradation of paracetamol mediating luminous textile: Intensification of the chemical oxidation. *Journal of Water Process Engineering*, 53, 103648. <https://doi.org/10.1016/J.JWPE.2023.103648>
- Dolatabadi, M., & Ahmadzadeh, S. (2019). A rapid and efficient removal approach for degradation of metformin in pharmaceutical wastewater using electro-Fenton process; optimization by response surface methodology. *Water Science and Technology*, 80(4), 685–694. <https://doi.org/10.2166/WST.2019.312>
- Dotto, G. L., & McKay, G. (2020). Current scenario and challenges in adsorption for water treatment. *Journal of Environmental Chemical Engineering*, 8(4), 103988. <https://doi.org/10.1016/J.JECE.2020.103988>
- Elmouwahidi, A., Bailón-García, E., Pérez-Cadenas, A. F., Maldonado-Hódar, F. J., & Carrasco-Marín, F. (2017). Activated carbons from KOH and H₃PO₄-activation of olive residues and its application as supercapacitor electrodes. *Electrochimica Acta*, 229, 219–228. <https://doi.org/10.1016/j.electacta.2017.01.152>
- Farooq, U., Sajid, M., Shan, A., Wang, X., & Lyu, S. (2021). Role of cysteine in enhanced degradation of trichloroethane under ferrous percarbonate system. *Chemical*

- Engineering Journal*, 423. <https://doi.org/10.1016/J.CEJ.2021.130221>
- Foo, K. Y., & Hameed, B. H. (2010). Insights into the modeling of adsorption isotherm systems. *Chemical Engineering Journal*, 156(1), 2–10. <https://doi.org/10.1016/J.CEJ.2009.09.013>
- Fu, F., & Wang, Q. (2011). Removal of heavy metal ions from wastewaters: A review. *Journal of Environmental Management*, 92(3), 407–418. <https://doi.org/10.1016/J.JENVMAN.2010.11.011>
- Garba, Z. N., Zhou, W., Lawan, I., Xiao, W., Zhang, M., Wang, L., et al. (2019). An overview of chlorophenols as contaminants and their removal from wastewater by adsorption: A review. *Journal of Environmental Management*, 241, 59–75. <https://doi.org/10.1016/J.JENVMAN.2019.04.004>
- Gayathiri, M., Pulingam, T., Lee, K. T., & Sudesh, K. (2022). Activated carbon from biomass waste precursors: Factors affecting production and adsorption mechanism. *Chemosphere*, 294, 133764. <https://doi.org/10.1016/J.CHEMOSPHERE.2022.133764>
- Gómez, M. J., Martínez Bueno, M. J., Lacorte, S., Fernández-Alba, A. R., & Agüera, A. (2007). Pilot survey monitoring pharmaceuticals and related compounds in a sewage treatment plant located on the Mediterranean coast. *Chemosphere*, 66(6), 993–1002. <https://doi.org/10.1016/J.CHEMOSPHERE.2006.07.051>
- Gómez-Oliván, L. M., Galar-Martínez, M., Islas-Flores, H., García-Medina, S., & Sanjuan-Reyes, N. (2014). DNA damage and oxidative stress induced by acetylsalicylic acid in *Daphnia magna*. *Comparative Biochemistry and Physiology Part - c: Toxicology and Pharmacology*, 164, 21–26. <https://doi.org/10.1016/J.CBPC.2014.04.004>
- Guo, X., & Wang, J. (2019). A general kinetic model for adsorption: Theoretical analysis and modeling. *Journal of Molecular Liquids*, 288, 111100. <https://doi.org/10.1016/J.MOLLIQ.2019.111100>
- Gupta, V. K., Ali, I., & Mohan, D. (2003). Equilibrium uptake and sorption dynamics for the removal of a basic dye (basic red) using low-cost adsorbents. *Journal of Colloid and Interface Science*, 265(2), 257–264. [https://doi.org/10.1016/S0021-9797\(03\)00467-3](https://doi.org/10.1016/S0021-9797(03)00467-3)
- Hernández, F., Legua, P., Melgarejo-Sánchez, P., & Martínez Font, R. (2012). The pomegranate tree in the world: Its problems and uses Options Méditerranéennes. *Séries A: Mediterranean Seminars*, 103, 209–215. <https://doi.org/10.3/JQUERY-UIJS>
- Ioannidou, O., & Zabaniotou, A. (2007). Agricultural residues as precursors for activated carbon production-A review. *Renewable and Sustainable Energy Reviews*, 11(9), 1966–2005. <https://doi.org/10.1016/J.RSER.2006.03.013>
- Jaria, G., Calisto, V., Esteves, V. I., & Otero, M. (2022). Overview of relevant economic and environmental aspects of waste-based activated carbons aimed at adsorptive water treatments. *Journal of Cleaner Production*, 344, 130984. <https://doi.org/10.1016/j.jclepro.2022.130984>
- Jyothirmayee, D., Harika, T., & Reddy, V. K. (2015). Development of immediate release liquid fill formulations Google Akademik. *International Journal of Pharmaceutical Development & Technology*, 5, 75–82.
- Kahramanoglu, I. (2019). Trends in pomegranate sector: Production, postharvest handling and marketing. *International Journal of Agriculture Forestry and Life Sciences*, 3(2), 239–246.
- Karri, R. R., & Sahu, J. N. (2018). Modeling and optimization by particle swarm embedded neural network for adsorption of zinc (II) by palm kernel shell based activated carbon from aqueous environment. *Journal of Environmental Management*, 206, 178–191. <https://doi.org/10.1016/J.JENVMAN.2017.10.026>
- Karthikeyan, S., Sivakumar, B., & Sivakumar, N. (2010). Film and pore diffusion modeling for adsorption of reactive red 2 from aqueous solution on to activated carbon prepared from bio-diesel industrial waste. *Journal of Chemistry*, 7(SUPPL. 1), S175–S184. <https://doi.org/10.1155/2010/138684>
- Kim, J.-H., Lee, G., Park, J.-E., & Kim, S.-H. (2021). Limitation of K₂CO₃ as a chemical agent for upgrading activated carbon. *Processes*, 9(6), 1000. <https://doi.org/10.3390/pr9061000>
- Lee, W. J., Goh, P. S., Lau, W. J., Wong, K. C., Suzaimi, N. D., & Ismail, A. F. (2022). Tailoring the permeability and flux stability of forward osmosis membrane with tert-butylamine functionalized carbon nanotubes for paracetamol removal. *Journal of Environmental Chemical Engineering*, 10(3), 107977. <https://doi.org/10.1016/J.JECE.2022.107977>
- Li, D., Shao, H., Huo, Z., Xie, N., Gu, J., & Xu, G. (2021). Typical antibiotics in the receiving rivers of direct-discharge sources of sewage across Shanghai: Occurrence and source analysis. *RSC Advances*, 11(35), 21579–21587. <https://doi.org/10.1039/D1RA02510D>
- Lladó, J., Lao-Luque, C., Ruiz, B., Fuente, E., Solé-Sardans, M., & Dorado, A. D. (2015). Role of activated carbon properties in atrazine and paracetamol adsorption equilibrium and kinetics. *Process Safety and Environmental Protection*, 95, 51–59. <https://doi.org/10.1016/J.PSEP.2015.02.013>
- Lourenção, B. C., Medeiros, R. A., Rocha-Filho, R. C., Mazo, L. H., & Fatibello-Filho, O. (2009). Simultaneous voltammetric determination of paracetamol and caffeine in pharmaceutical formulations using a boron-doped diamond electrode. *Talanta*, 78(3), 748–752. <https://doi.org/10.1016/J.TALANTA.2008.12.040>
- Macías-García, A., García-Sanz-Calcedo, J., Carrasco-Amador, J. P., & Segura-Cruz, R. (2019). Adsorption of paracetamol in hospital wastewater through activated carbon filters. *Sustainability*, 11(9), 2672. <https://doi.org/10.3390/SU11092672>
- Meinan, X., Yimeng, W., Chao, W., Tianli, T., Li, J., Peng, Y., & Xiangping, N. (2022). Response of the Sirtuin/PXR signaling pathway in *Mugilogobius chulae* exposed to environmentally relevant concentration Paracetamol. *Aquatic Toxicology*, 249, 106222. <https://doi.org/10.1016/J.AQUATOX.2022.106222>
- Nadour, M., Boukraa, F., & Benaboura, A. (2019). Removal of diclofenac, paracetamol and metronidazole using a carbon-polymeric membrane. *Journal of Environmental Chemical Engineering*, 7(3), 103080. <https://doi.org/10.1016/J.JECE.2019.103080>
- Namvar-Mahboub, M., Ahsani, F., & Ansari, S. (2020). Preparation and characterization of nanosized pomegranate

- peel-based activated carbon for application in pyridine removal from aqueous solution. *Theoretical Foundations of Chemical Engineering*, 54(5), 940–948. <https://doi.org/10.1134/S0040579520050371/FIGURES/11>
- Nayeri, D., & Mousavi, S. A. (2020). Dye removal from water and wastewater by nanosized metal oxides - modified activated carbon: A review on recent researches. *Journal of Environmental Health Science and Engineering*, 18(2), 1671–1689. <https://doi.org/10.1007/S40201-020-00566-W>
- Omri, A., Benzina, M., & Ammar, N. (2013). Preparation, modification and industrial application of activated carbon from almond shell. *Journal of Industrial and Engineering Chemistry*, 19(6), 2092–2099. <https://doi.org/10.1016/J.JIEC.2013.03.025>
- Park, G. S. (1975). *The mathematics of diffusion* (2nd ed.). J. Crank Clarendon Press.
- Phong Vo, H. N., Le, G. K., Hong Nguyen, T. M., Bui, X. T., Nguyen, K. H., Rene, E. R., et al. (2019). Acetaminophen micropollutant: Historical and current occurrences, toxicity, removal strategies and transformation pathways in different environments. *Chemosphere*, 236. <https://doi.org/10.1016/J.CHEMOSPHERE.2019.124391>
- Pi, N., Ng, J. Z., & Kelly, B. C. (2017). Bioaccumulation of pharmaceutically active compounds and endocrine disrupting chemicals in aquatic macrophytes: Results of hydroponic experiments with *Echinodorus horemanii* and *Eichhornia crassipes*. *Science of the Total Environment*, 601–602, 812–820. <https://doi.org/10.1016/J.SCITOTENV.2017.05.137>
- Puziy, A. M., Poddubnaya, O. I., Martínez-Alonso, A., Suárez-García, F., & Tascón, J. M. D. (2005). Surface chemistry of phosphorus-containing carbons of lignocellulosic origin. *Carbon*, 43(14), 2857–2868. <https://doi.org/10.1016/J.CARBON.2005.06.014>
- Qian, W., Sun, F., Xu, Y., Qiu, L., Liu, C., Wang, S., & Yan, F. (2013). Human hair-derived carbon flakes for electrochemical supercapacitors. *Energy & Environmental Science*, 7(1), 379–386. <https://doi.org/10.1039/C3EE43111H>
- Ramutshatsha-Makhwedzha, D., Mavhungu, A., Moropeng, M. L., & Mbaya, R. (2022). Activated carbon derived from waste orange and lemon peels for the adsorption of methyl orange and methylene blue dyes from wastewater. *Helvion*, 8(8), e09930. <https://doi.org/10.1016/J.HELIVION.2022.E09930>
- Roberts, P. H., & Thomas, K. V. (2006). The occurrence of selected pharmaceuticals in wastewater effluent and surface waters of the lower Tyne catchment. *Science of the Total Environment*, 356(1–3), 143–153. <https://doi.org/10.1016/J.SCITOTENV.2005.04.031>
- Saad, M. J., Sajab, M. S., Wan Busu, W. N., Misran, S., Zakaria, S., Chin, S. X., & Chia, C. H. (2020). Comparative adsorption mechanism of rice straw activated carbon activated with NaOH and KOH. *Sains Malaysiana*, 49(11), 2721–2734. <https://doi.org/10.17576/jsm-2020-4911-11>
- Saadi, W., Rodríguez-Sánchez, S., Ruiz, B., Najjar-Souissi, S., Ouederni, A., & Fuente, E. (2022). From pomegranate peels waste to one-step alkaline carbonate activated carbons. Prospect as sustainable adsorbent for the renewable energy production. *Journal of Environmental Chemical Engineering*, 10(1), 107010. <https://doi.org/10.1016/J.JECE.2021.107010>
- Sahoo, T. R., & Prelot, B. (2020). Nanomaterials for the detection and removal of wastewater pollutants. In Barbara Bonelli, Francesca S. Freyria, R. Ilenia, & Rajandrea Seth (Eds.), *Nanomaterials for the Detection and Removal of Wastewater Pollutants* (Elsevier., pp. 161–222). Elsevier. <https://doi.org/10.1016/B978-0-12-818489-9.00007-4>
- Senthilkumar, T., Chattopadhyay, S. K., & Miranda, L. R. (2016). Optimization of activated carbon preparation from pomegranate peel (*Punica granatum Peel*) using RSM. *Chemical Engineering Communications*, 204(2), 238–248. <https://doi.org/10.1080/00986445.2016.1262358>
- Shokoohi, R., Samadi, M. T., Amani, M., & Poureshgh, Y. (2018). Optimizing laccase-mediated amoxicillin removal by the use of box–behnen design in an aqueous solution. *Desalination and Water Treatment*, 119, 53–63. <https://doi.org/10.5004/DWT.2018.21922>
- Solmaz, A., Karta, M., Depci, T., Turna, T., & Sari, Z. A. (2023). Preparation and characterization of activated carbons from lemon pulp for oxytetracycline removal. *Environmental Monitoring and Assessment*, 195(7), 797. <https://doi.org/10.1007/s10661-023-11421-4>
- Soltani, R. D. C., Miraftebi, Z., Mahmoudi, M., Jorfi, S., Boczkaj, G., & Khataee, A. (2019). Stone cutting industry waste-supported zinc oxide nanostructures for ultrasonic assisted decomposition of an anti-inflammatory non-steroidal pharmaceutical compound. *Ultrasonics Sonochemistry*, 58. <https://doi.org/10.1016/J.ULTSONCH.2019.104669>
- Spessato, L., Bedin, K. C., Cazetta, A. L., Souza, I. P. A. F., Duarte, V. A., Crespo, L. H. S., et al. (2019). KOH-super activated carbon from biomass waste: Insights into the paracetamol adsorption mechanism and thermal regeneration cycles. *Journal of Hazardous Materials*, 371, 499–505. <https://doi.org/10.1016/J.JHAZMAT.2019.02.102>
- Tran, H. N., Tomul, F., Ha, N. T., Nguyen, D. T., Lima, E. C., Le, G. T., Chang, C. T., Masindi, V., Woo, S. H., et al. (2020). Innovative spherical biochar for pharmaceutical removal from water: Insight into adsorption mechanism. *Journal of Hazardous Materials*, 394, 122255. <https://doi.org/10.1016/J.JHAZMAT.2020.122255>
- Tunç Sara, M., Yıldız, B., & Taşar, Ş. (2021). Removal of paracetamol from aqueous solution by wood sawdust-derived activated carbon: Process optimization using response surface methodology. *Chemical Engineering Communications*, 209(8), 1130–1150. <https://doi.org/10.1080/00986445.2021.1978075>
- Turkmen Koc, S. N., Kipcak, A. S., MoroydorDerun, E., & Tugrul, N. (2021). Removal of zinc from wastewater using orange, pineapple and pomegranate peels. *International Journal of Environmental Science and Technology*, 18(9), 2781–2792. <https://doi.org/10.1007/S13762-020-03025-Z/FIGURES/8>
- Vaiano, V., Matarangolo, M., & Sacco, O. (2018). UV-LEDs floating-bed photoreactor for the removal of caffeine and paracetamol using ZnO supported on polystyrene pellets. *Chemical Engineering Journal*, 350, 703–713. <https://doi.org/10.1016/J.CEJ.2018.06.011>
- Wang, J., & Guo, X. (2020). Adsorption kinetic models: Physical meanings, applications, and solving methods. *Journal of Hazardous Materials*, 390, 122156.
- Weber, W. J., Jr., & Morris, J. C. (1963). Kinetics of adsorption on carbon from solution. *Journal of the Sanitary*

- Engineering Division*, 89(2), 31–59. <https://doi.org/10.1061/JSEDAI.0000430>
- Wu, S., Zhang, L., & Chen, J. (2012). Paracetamol in the environment and its degradation by microorganisms. *Applied Microbiology and Biotechnology*, 96(4), 875–884. <https://doi.org/10.1007/s00253-012-4414-4>
- Yahya, M. A., Al-Qodah, Z., & Ngah, C. W. Z. (2015). Agricultural bio-waste materials as potential sustainable precursors used for activated carbon production: A review. *Renewable and Sustainable Energy Reviews*, 46, 218–235. <https://doi.org/10.1016/J.RSER.2015.02.051>
- Yun, W. C., Lin, K. Y. A., Tong, W. C., Lin, Y. F., & Du, Y. (2019). Enhanced degradation of paracetamol in water using sulfate radical-based advanced oxidation processes catalyzed by 3-dimensional Co₃O₄ nanoflower. *Chemical Engineering Journal*, 373, 1329–1337. <https://doi.org/10.1016/J.CEJ.2019.05.142>
- Zarroug, M., Najjar-Souissi, S., Menéndez, J. A., Calvo, E. G., & Ouederni, A. (2022). Fast production of activated carbon from pomegranate peels by combining microwave heating and phosphoric acid activation for paracetamol adsorption. <https://home.liebertpub.com/ees>, 39(5), 441–452. <https://doi.org/10.1089/EES.2021.0125>
- Zein, S. H., & Antony, A. (2022). Techno-economic analysis and feasibility of industrial-scale activated carbon production from agricultural pea waste using microwave-assisted pyrolysis: A circular economy approach. *Processes*, 10(9), 1702. <https://doi.org/10.3390/pr10091702>
- Zhang, L., Wang, Q., Wang, B., Yang, G., Lucia, L. A., & Chen, J. (2015). Hydrothermal carbonization of corncob residues for hydrochar production. *Energy and Fuels*, 29(2), 872–876. <https://doi.org/10.1021/EF502462P>
- Zhou, Y. L., Zhang, Q., Yu, Y. B., Wang, B. X., & Hong, J. M. (2021). Active precursor-induced high-content graphitic-N-doped graphene oxide for the electrocatalytic degradation of paracetamol. *Applied Surface Science*, 542, 148753. <https://doi.org/10.1016/J.APSUSC.2020.148753>
- Žur, J., Wojcieszynska, D., Hupert-Kocurek, K., Marchlewicz, A., & Guzik, U. (2018). Paracetamol – Toxicity and microbial utilization. *Pseudomonas moorei* KB4 as a case study for exploring degradation pathway. *Chemosphere*, 206, 192–202. <https://doi.org/10.1016/J.CHEMOSPHERE.2018.04.179>

Publisher's Note Springer Nature remains neutral with regard to jurisdictional claims in published maps and institutional affiliations.

Springer Nature or its licensor (e.g. a society or other partner) holds exclusive rights to this article under a publishing agreement with the author(s) or other rightsholder(s); author self-archiving of the accepted manuscript version of this article is solely governed by the terms of such publishing agreement and applicable law.